

 Open access • Journal Article • DOI:10.1039/C2DT12190E

Re-dispersion and film formation of GdVO₄ : Ln³⁺ (Ln³⁺ = Dy³⁺, Eu³⁺, Sm³⁺, Tm³⁺) nanoparticles: particle size and luminescence studies. — [Source link](#)

N. Shanta Singh, Raghumani Singh Ningthoujam, Ganngam Phaomei, S. Dorendrajit Singh ...+2 more authors


Institutions: Manipur University, Bhabha Atomic Research Centre, National Institute for Materials Science

Published on: 21 Mar 2012 - Dalton Transactions (The Royal Society of Chemistry)

Topics: Luminescence, Nucleation, Aqueous solution, Crystallite and Particle size

Related papers:

- [Size-induced variations in bulk/surface structures and their impact on photoluminescence properties of GdVO₄:Eu³⁺ nanoparticles.](#)
- [Multifunctional Eu³⁺- and Er³⁺/Yb³⁺-doped GdVO₄ nanoparticles synthesized by reverse micelle method](#)
- [Lanthanide-doped GdVO₄ upconversion nanophosphors with tunable emissions and their applications for biomedical imaging](#)
- [Revised effective ionic radii and systematic studies of interatomic distances in halides and chalcogenides](#)
- [Preparation of white light emitting YVO₄: Ln³⁺ and silica-coated YVO₄:Ln³⁺ \(Ln³⁺ = Eu³⁺, Dy³⁺, Tm³⁺\) nanoparticles by CTAB/n-butanol/hexane/water microemulsion route: Energy transfer and site symmetry studies](#)

Share this paper:    

View more about this paper here: <https://typeset.io/papers/re-dispersion-and-film-formation-of-gdvo4-ln3-ln3-dy3-eu3-3zvevh565b>

Re-dispersion and film formation of $\text{GdVO}_4 : \text{Ln}^{3+}$ ($\text{Ln}^{3+} = \text{Dy}^{3+}, \text{Eu}^{3+}, \text{Sm}^{3+}, \text{Tm}^{3+}$) nanoparticles: particle size and luminescence studies†N. Shanta Singh,^a R. S. Ningthoujam,^{*b} Ganngam Phaomei,^c S. Dorendrajit Singh,^a A. Vinu^d and R. K. Vatsa^b

Received 16th November 2011, Accepted 6th January 2012

DOI: 10.1039/c2dt12190e

$\text{GdVO}_4 : \text{Ln}^{3+}$ ($\text{Ln}^{3+} = \text{Dy}^{3+}, \text{Eu}^{3+}, \text{Sm}^{3+}, \text{Tm}^{3+}$) nanoparticles are prepared by a simple chemical route at 140 °C. The crystallite size can be tuned by varying the pH of the reaction medium. Interestingly, the crystallite size is found to increase significantly when pH increases from 6 to 12. This is related to slower nucleation of the GdVO_4 formation with increase of VO_4^{3-} present in solution. The luminescence study shows an efficient energy transfer from vanadate absorption of GdVO_4 to Ln^{3+} and thereby enhanced emissions are obtained. A possible reaction mechanism at different pH values is suggested in this study. As-prepared samples are well dispersed in ethanol, methanol and water, and can be incorporated into polymer films. Luminescence and its decay lifetime studies confirm the decrease in non-radiative transition probability with the increase of heat treatment temperature. Re-dispersed particles will be useful in potential applications of life science and the film will be useful in display devices.

1. Introduction

Luminescent materials based on the lanthanide ion (Ln^{3+}) emission have vast applications in phosphor lamps and display devices,¹ cathode ray tubes,^{1,2} components of telecommunication³ as well as active laser materials.⁴ Recently there has been great interest in the incorporation of these luminescent materials in the polymer based materials because of easy processing of polymers and ease of integrating different components. With the recent developments in the high resolution flat panel display and field emission displays, the demand for stable and highly bright luminescent materials has increased. In this context, there are many potential host materials such as GdVO_4 , Y_2O_3 , YVO_4 , Gd_2O_3 , LaPO_4 , YPO_4 , GdPO_4 , *etc.*^{5–23} Among these materials, GdVO_4 is an interesting and excellent host material for lanthanide ion emission such as Eu^{3+} , Dy^{3+} , Sm^{3+} , Tm^{3+} , *etc.* for two reasons: (a) efficient energy transfer (ET) from the VO_4^{3-} (vanadate) absorption to the excited states of the activators (Ln^{3+}) and

(b) Gd^{3+} ($4f^7$) has a strong absorption peak at ~280 nm ($S \rightarrow I$ transition)¹ and thereby energy transfer (CT) is possible to the excited states of the activators (Ln^{3+}).

Many of these potential phosphors are synthesized either at high temperature or by post annealing at high temperature. Such methods of preparation lead to a micron size and agglomerated nanosized particles. This gives rise to formation of particles without organic–inorganic groups on the surface and therefore they are poor dispersants in solvents. This makes it difficult to incorporate them in polymer based films. In some cases in where Ln^{3+} ions can not form a solid solution with the host, clustering of Ln^{3+} ions occurs on the grain boundary during heating the samples at higher temperature or sintering, and thereby the luminescence intensity decreases due to cross-relaxation among Ln^{3+} ions.

In recent years, low temperature synthesis using colloidal chemistry has been used successfully to prepare well-dispersed nanoparticles with a controlled size, shape, and surface state. The potential of this method has been exploited for the preparation of II–VI semiconductor nanoparticles with very narrow size distribution and a luminescence quantum yield up to 60%.^{24–26} Riwotzki and Haase prepared the nanoparticles of YVO_4 at 200 °C using the hydrothermal technique.^{12,13} In addition, there are many other methods such as the sol gel method, urea precipitation, the co-precipitation method, *etc.* The wet chemical method using appropriate organic–inorganic ligands is one of the convenient ways to stabilize the growth of nanoparticles for preparing nearly monodisperse particles. Moreover, good dispersion of the particles in a particular solvent is generally achieved by organic groups present on the surface of the particles. However, long chain organic ligands lead to the quenching of luminescence due to the high energy vibrations of

^aDepartment of Physics, Manipur University, Canchipur, Imphal-795003, Manipur, India. E-mail: dorendrajit@yahoo.co.in

^bChemistry Division, Bhabha Atomic Research Centre, Mumbai-400085, India. E-mail: rsn@barc.gov.in; Fax: +91 22 25505151; Tel: +91 22 25592321

^cDepartment of Chemistry, Manipur University, Canchipur, Imphal-795003, Manipur, India

^dNational Institute for Materials Science 1-1, Namiki, Tsukuba, Japan

†Electronic supplementary information (ESI) available: XRD patterns of as-prepared, 500 and 900 °C heated samples of GdVO_4 samples doped with (a) 1, (b) 5, (c) 7, (d) 10 and (e) 15 at.% Sm^{3+} , luminescence spectra of as-prepared samples after dispersion in methanol and water, FTIR spectra of PVA films and luminescence spectra of 500 and 900 °C annealed GdVO_4 samples doped with (a) Dy^{3+} (2 at.%), (b) Eu^{3+} (5 at.%) and (c) Tm^{3+} (2 at.%) are available. See DOI: 10.1039/c2dt12190e

the ligands. In this regard, the choice of organic ligands having a short chain like ethylene glycol (EG) or polyethylene glycol (PEG) becomes important for the preparation of such phosphor materials which can be dispersed in solvents such as methanol, ethanol, water, *etc.* These dispersed particles can then be incorporated in the polymer based materials. Moreover, EG and PEG have an additional advantage in terms of cost and can be easily removed by heat treatment at around 500 °C, as well as the preparation can be carried out at relatively low temperature without any special precautions.

The preparation of Ln^{3+} doped GdVO_4 nanoparticles at low temperature using a short chain capping agent and NaOH as a hydrolyzing agent has not been reported so far in the literature. In this report, we have prepared re-dispersible particles of GdVO_4 doped with Eu^{3+} (5 at.%), Dy^{3+} (2 at.%), Sm^{3+} (1–15 at.%) and Tm^{3+} (2 at.%) using EG and PEG at low temperature. NaOH is used as a hydrolyzing agent and its role at varying pH is discussed. The present investigation reports a systematic study of the pH dependence on the crystallinity of GdVO_4 particles. The samples were characterized using X-ray diffraction (XRD), IR, UV-visible spectroscopy and transmission electron microscopy (TEM). The luminescent properties and the decay processes of the as-prepared samples and heated samples at different temperatures are also reported.

Additionally, homogeneous dispersion of the samples in polar solvents such as water, methanol, ethanol, *etc.* as well as incorporation of the samples in polyvinyl alcohol (PVA) for polymer based films is also investigated.

2. Experimental details

2.1 Materials

All chemicals are of analytical grade and used as received. Gadolinium oxide (Gd_2O_3 , 99.99%, Alfa Aesar), ammonium metavanadate (NH_4VO_3 , 99.99%, Aldrich), dysprosium carbonate ($\text{Dy}_2(\text{CO}_3)_3 \cdot 4\text{H}_2\text{O}$, 99.99% Alfa Aesar), europium oxide (Eu_2O_3 , 99.9% Aldrich), samarium oxide (Sm_2O_3 , 99.9% Aldrich) and thulium oxide (Tm_2O_3 , 99.9% Aldrich) were used as sources of Gd^{3+} , VO_4^{3-} , Dy^{3+} , Eu^{3+} , Sm^{3+} and Tm^{3+} , respectively. PEG-1000 (Fluka), EG, sodium hydroxide (NaOH) and nitric acid (HNO_3) were used without further purification.

2.2 Preparation of Sm^{3+} , Eu^{3+} , Tm^{3+} or Dy^{3+} doped GdVO_4 nanoparticles

GdVO_4 nanoparticles doped with Sm^{3+} (Sm^{3+} = 1, 3, 5, 7, 10 and 15 at.%) were prepared by the wet chemical method using PEG and EG at 140 °C for 2 h. In a typical synthesis of 3 at.% Sm^{3+} doped GdVO_4 nanoparticles, 500 mg of Gd_2O_3 and 25 mg of Sm_2O_3 were dissolved together in 3 ml of conc. HNO_3 (16 M) in a 100 ml two-necks round-bottom flask. The excess acid was removed by evaporation with distilled water (15 ml). Here, Gd^{3+} ions exist and the pH was found to be 1.1. To this reaction medium, 50 ml of EG and 3 g of PEG were added. Three hundred and forty milligrams of NH_4VO_3 was dissolved in 3 ml of conc. NaOH (3.2 M) and its pH was found to be 13, in which VO_3^- ions are converted into VO_4^{3-} ions.^{27,28} The solution containing Gd^{3+} was treated with a solution containing VO_4^{3-} and its pH was found to be 6. The pH was increased to 12 after an

addition of NaOH solution. The reaction was carried out at 140 °C for 2 h. The precipitates formed were separated by centrifugation and washed three times with doubly distilled water in order to remove the excess EG and PEG. A similar procedure was followed for all Sm^{3+} doped GdVO_4 samples using stoichiometric amounts of the constituents. Following a similar process, Eu^{3+} (5 at.%) or Dy^{3+} (2 at.%) or Tm^{3+} (2 at.%) doped GdVO_4 sample was prepared. Further, all the Sm^{3+} doped samples were heated under ambient conditions at different temperatures of 500–900 °C in order to see the effect of the heat treatment. The duration of the heat treatment for each sample was 4 h.

2.3 Preparation of 5 at.% Eu^{3+} doped GdVO_4 nanoparticles at different pH values

As mentioned above, we used 25 mg of Eu_2O_3 instead of Sm_2O_3 . The mixing of Gd^{3+} – Eu^{3+} ions with VO_4^{3-} gave pH = 6 and the precipitate was collected. The samples obtained at pH = 9, 10, 11, 12 and 13 were prepared after addition of NaOH solution. Initially, the nucleation of GdVO_4 formation is fast in the presence of Gd^{3+} and VO_4^{3-} ions when pH = 6–7, however the particle growth is hindered, resulting in a smaller size of the particle because part of VO_4^{3-} will be converted to VO_2^{+} .^{28,29} Above pH 8, some part of Gd^{3+} and VO_4^{3-} will be in the form of $\text{Gd}(\text{OH})_3$ and $\text{VO}_3(\text{OH})^{2-}$ species, respectively²⁹ and thus, the nucleation is still slow, but the growth increases. When pH = 12–13, only the VO_4^{3-} ions are retained.³⁰ The formation of GdVO_4 is high and the particle growth is high.

2.4 Characterization

X-Ray diffraction measurements of all the samples were carried out using Philips X-ray diffractometer (PW 1071) with $\text{CuK}\alpha$ (1.5405 Å) radiation having a Ni filter. The average crystallite size (d) was calculated using the Debye–Scherrer relation, $d = 0.9\lambda/\beta \cos \theta$ where λ is the wavelength of the X-ray and β is the full width at half maximum intensity. Fourier transform infrared (FT-IR) spectroscopy studies were carried out using a Shimadzu (model 8400S) spectrophotometer. The transmission electron microscopy (TEM) images were recorded using JEOL FX 2000 microscope. The sample for TEM measurement was prepared by dispersing in methanol and ultrasonication for 20 min. The dispersed particles were put over a 200 mesh carbon coated copper grid and dried in ambient atmosphere. A UV-visible absorption spectrum was recorded using Perkin Elmer Lambda 35.

All luminescence spectra and their decay data were recorded using EDINBURGH instrument FLS920 equipped with 450 W Xenon arc lamp having Peltier element cooled red sensitive Hamamatsu R955 PMT and a microsecond flash lamp (100 W). The samples were prepared by dispersing in methanol, spreading over the quartz slide and drying in ambient atmosphere.

3. Results and discussion

3.1 XRD study

XRD patterns of (a) Dy^{3+} (2 at.%), (b) Eu^{3+} (5 at.%), (c) Sm^{3+} (3 at.%) and (d) Tm^{3+} (2 at.%) doped as-prepared GdVO_4

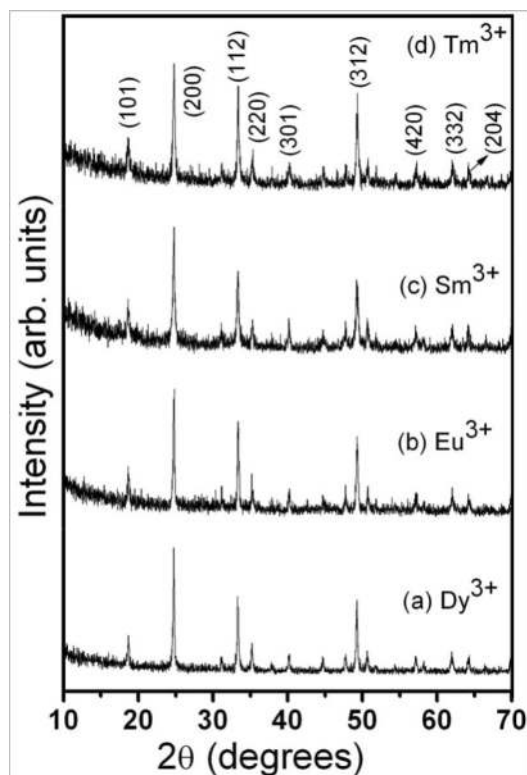


Fig. 1 X-Ray diffraction patterns of as-prepared GdVO_4 doped with (a) Dy^{3+} (2 at.%), (b) Eu^{3+} (5 at.%), (c) Sm^{3+} (3 at.%) and (d) Tm^{3+} (2 at.%). Here all samples were prepared at pH = 12.

samples (pH = 12) are shown in Fig. 1 and the samples are found to be crystalline belonging to a tetragonal zircon type structure of GdVO_4 (some prominent peaks in the patterns are assigned; JCPDS no. 17-0260). The crystallite sizes estimated using the Debye–Scherrer relation are found to be 40, 34, 33, and 35 nm for Dy^{3+} , Eu^{3+} , Sm^{3+} , and Tm^{3+} doped GdVO_4 , respectively. Possible oxide phases such as Gd_2O_3 , Dy_2O_3 , Eu_2O_3 , Sm_2O_3 , and Tm_2O_3 are absent in all XRD patterns. Also, other $\text{Gd}_8\text{V}_2\text{O}_{17}$ and GdV_3O_9 phases have not been found. This is an indication of the substitution of dopant ions in Gd sites of GdVO_4 tetragonal structure. Improvement in crystallinity is found in heating the as-prepared samples (pH = 12) up to 900 °C (see ESI, Fig. S1–S3†). Here Sm^{3+} (1–15 at.%) doped GdVO_4 samples are taken as examples and their luminescence properties will be discussed later.

Fig. 2(a) shows the XRD patterns of $\text{GdVO}_4:\text{Eu}^{3+}$ (5 at.%) samples prepared at different pH levels at the start of the reaction. The pH values measured at the end of the reaction are found to be lower than the starting pH value by about 0.6 to 0.8. All samples are crystalline in nature, belonging to the tetragonal structure of GdVO_4 irrespective of the pH values of the reaction medium. Interestingly, at pH = 6, the peaks are very broad indicating nanocrystallinity and the crystallite size is very small (6 nm). With the increase of pH, broadening of the peak decreases. At or above pH = 12, the peak broadening remains constant. The crystallite sizes of the systems with pH = 9, 10, 11, 12 and 13 are found to be 8, 10, 16, 34 and 33 nm, respectively, within an error of ± 2 nm. This has been shown in Fig. 2 (b), in which the growth of nanoparticles is enhanced

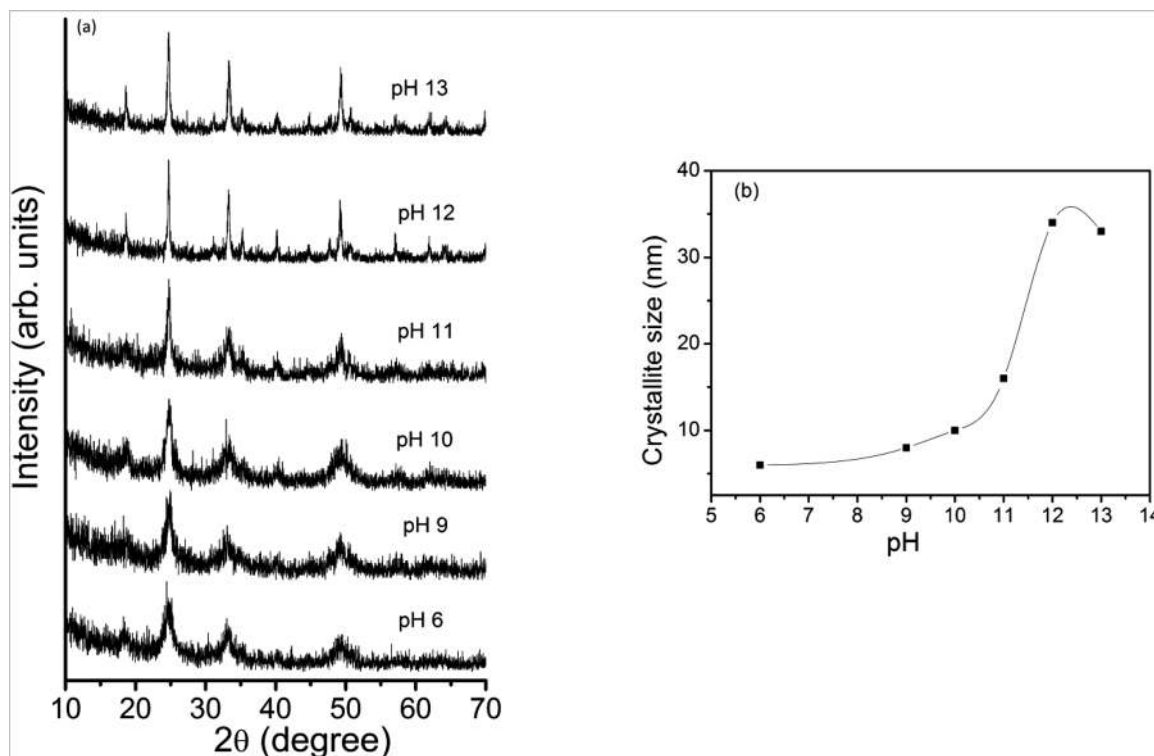


Fig. 2 (a) X-Ray diffraction patterns of $\text{GdVO}_4:\text{Eu}^{3+}$ (5 at.%) samples prepared at different pH levels at the start of the reaction and (b) crystallite size vs. pH.

significantly when the pH increases from 10 to 12. A similar observation was reported by Sun *et al.*³¹ during the preparation of YVO_4 in which the particle size changes from 14 to 47 nm when the pH changes from 9 to 10. However, no explanation was given. As can be seen from the XRD patterns, the particle size can be controlled by a simple change of pH.

3.2 TEM and EDX studies

Fig. 3 shows the TEM images of $\text{GdVO}_4 : \text{Eu}^{3+}$ (5 at.%) samples prepared at different pH values of (a) 6, (b) 9, (c) 10, and (d) 12. For pH values of 6 and 9, the particles are spherical in shape. The particle size increases from 8 to 15 nm when the pH changes from 6 to 9. Since particle size is small for pH 6 and 9, their high resolution TEM images are shown in Fig. 3(a) and (b). The morphology of the particles changes from spherical to

cuboid like the shape when the samples are prepared at pH 10. The particle size is found to be 30–40 nm. With further increase of pH of the reaction medium up to 12, the particle size of the cuboid shape increases. The particle size is found to be 60–80 nm. The particle size distributions for pH 10 and 12 are given on the left side of Fig. 3(c) and (d). Increase of particle size is found when pH increases from 6 to 12. The possible mechanism has been explained in the preparation section of 5 at. % Eu^{3+} doped GdVO_4 nanoparticles at different pH values. Change of the particle shape from spherical to cuboid may be related to the anisotropy nature induced by OH^- ions, which are available in excess at higher pH.

Fig. 4 shows a TEM image of the $\text{GdVO}_4 : \text{Sm}^{3+}$ (3 at.%) particles prepared at pH = 12 along with particle size distribution. There are the cuboid-shaped particles having a particle size ~60 nm without much interaction among them. Fig. 5 shows the

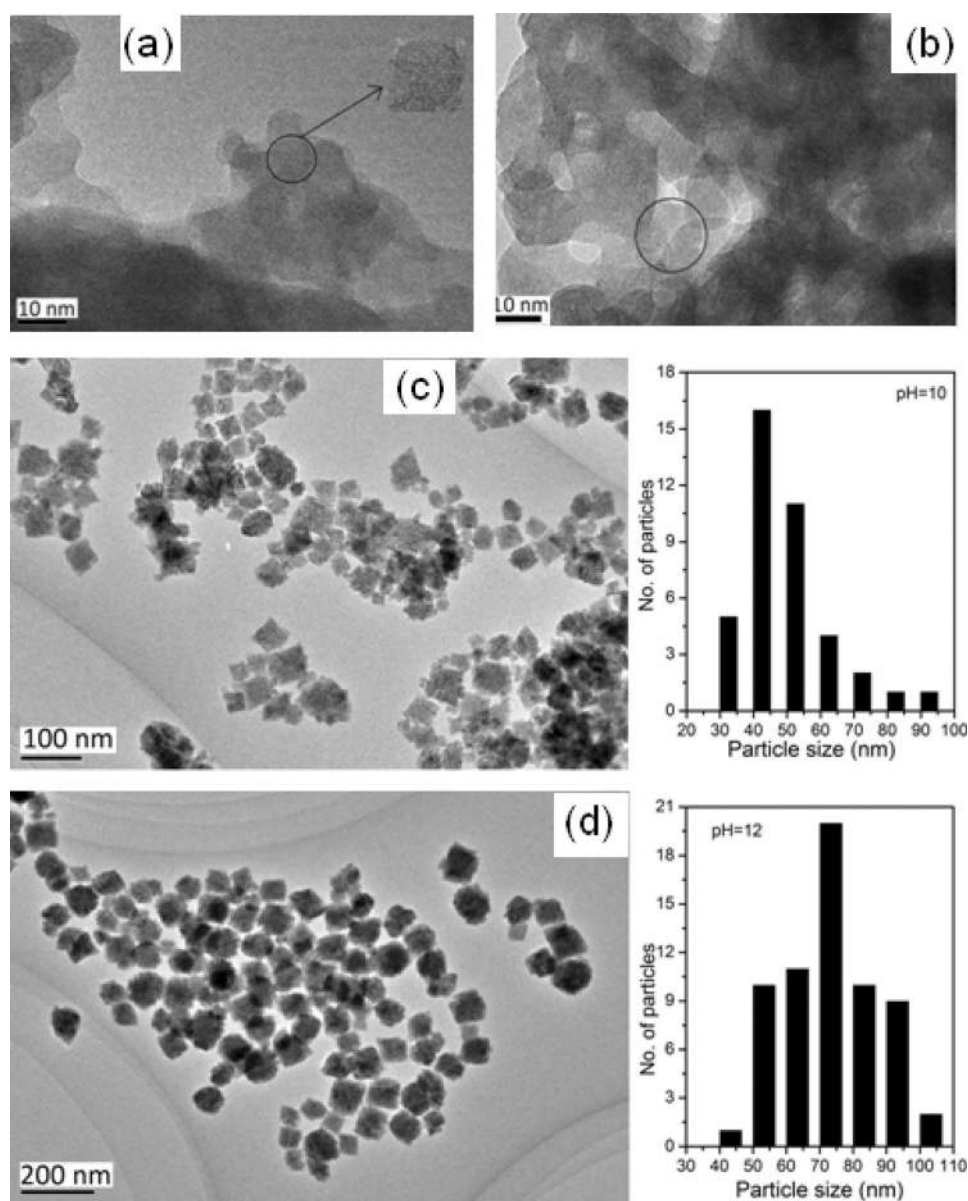


Fig. 3 TEM images of $\text{GdVO}_4 : \text{Eu}^{3+}$ (5 at.%) samples prepared at pH (a) 6, (b) 9, (c) 10 (d) 12 along with the particle size distributions of pH 10 and 12.

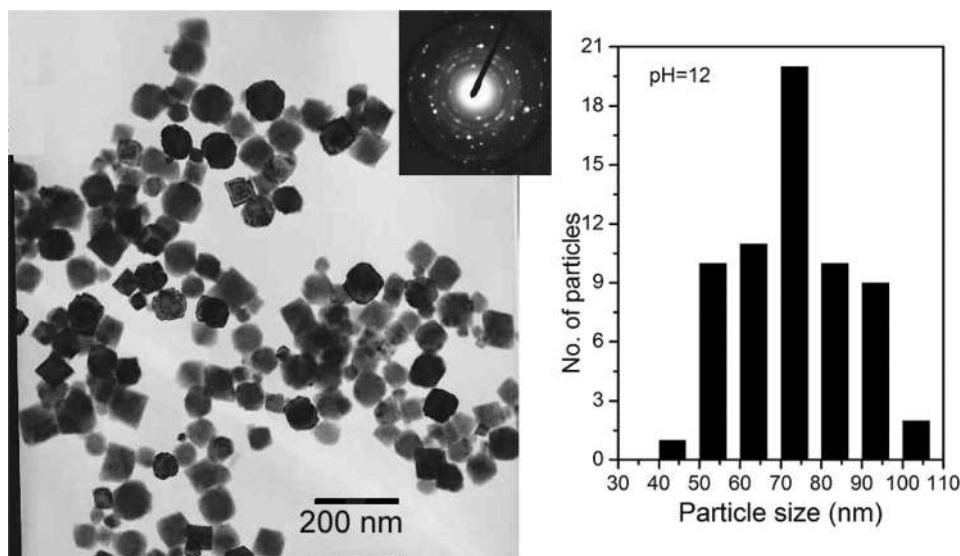


Fig. 4 TEM images of a $\text{GdVO}_4 : \text{Sm}^{3+}$ (3 at.%) sample prepared at pH 12 along with SAED pattern and particle size distribution.

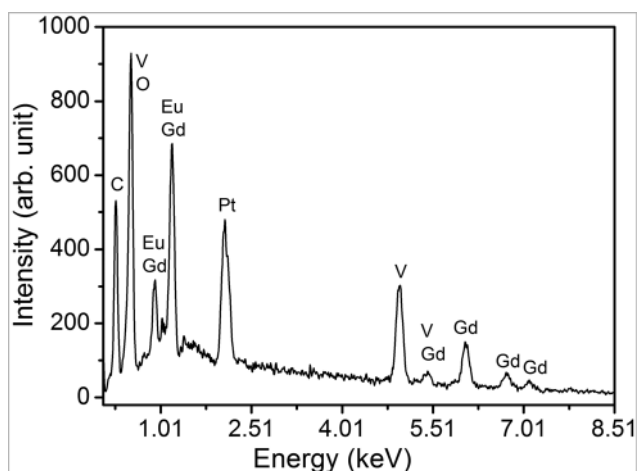


Fig. 5 EDAX spectrum of $\text{GdVO}_4 : \text{Eu}^{3+}$ (5 at.%) prepared at pH = 12.

EDX spectrum of $\text{GdVO}_4 : \text{Eu}^{3+}$ (5 at.%) prepared at pH = 12. The observed values of Gd, Eu and V are found to be 47, 3 and 54 at.%, respectively. The respective theoretical calculated values of Gd, Eu and V are 47.5, 2.5, and 50 at.%, respectively.

3.3 FTIR study

Fig. 6(a) shows the FTIR spectra of the as-prepared samples (pH = 12) of (i) Dy^{3+} (2 at.%), (ii) Eu^{3+} (5 at.%), (iii) Sm^{3+} (3 at.%) and (iv) Tm^{3+} (2 at.%) doped GdVO_4 . Samples show a peak around 470 cm^{-1} which attributes to Gd–O vibration mode and peak around 810 cm^{-1} is characteristic of V–O bond vibration.^{5,6,14} A shoulder peak at 1645 and 3420 cm^{-1} can be attributed to –OH bending and stretching vibrations arising from EG–PEG or water absorption. However, the stretching frequency of free –OH occurs at 3650 cm^{-1} . In this study, a red shifted broad band at 3420 cm^{-1} is an indication of the presence of a hydrogen bond in EG–PEG molecules. The weak peaks observed at 2858 and 2925 cm^{-1} are attributed to the CH_2

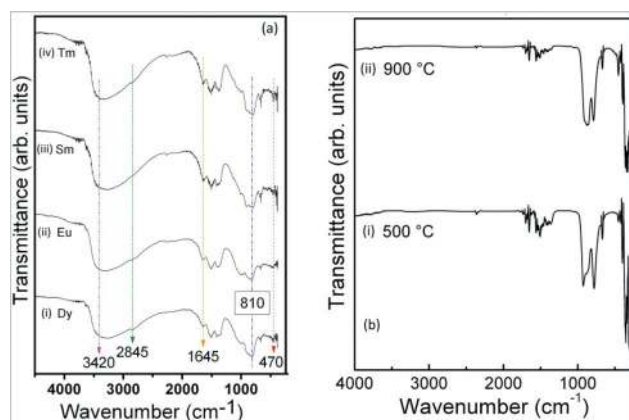


Fig. 6 FTIR spectra of (a) as-prepared GdVO_4 doped with (i) Dy^{3+} (2 at.%), (ii) Eu^{3+} (5 at.%), (iii) Sm^{3+} (3 at.%) and (iv) Tm^{3+} (2 at.%) and (b) $\text{GdVO}_4 : \text{Eu}^{3+}$ (5 at.%) (pH = 12) annealed at 500 and 900°C .

stretching vibrations arising from EG–PEG and these peaks are dominated by a strong peak of –OH stretching vibration. Fig. 6 (b) shows the FTIR spectra of a sample (5 at.% Eu^{3+} doped GdVO_4 prepared at pH = 12) annealed at 500 and 900°C . The presence of organic groups such as CH_2 band has not been observed. The intensity of the bending vibration of OH decreases drastically and its stretching vibration almost disappears in the 900°C annealed sample.

3.4 UV-visible absorption study

Fig. 7 shows UV-visible absorption spectra of 5 at.% Eu^{3+} doped GdVO_4 samples prepared at different pH = 6, 9, 10 and 12. The samples are dispersed in methanol (about $0.2\text{--}0.5 \text{ mg ml}^{-1}$). A broad peak in the range 250–350 nm is observed. This is related to the V–O charge transfer (CT). The Eu–O CT expected in the region of 250–260 nm could not be observed distinctly due to overlapping with the V–O CT band. Also, transitions due to the Eu^{3+} in the range of 300–500 nm could not be

observed due to quenching. A gradual red shift in the absorption peak is observed with the increase in the pH of the reaction; *e.g.* the absorption peaks of samples prepared at pH = 6 and 12 are found at 278 and 288 nm, respectively. This is related to the particle size effect. In addition to this, small size nanoparticles also have dangling bonds between V and O and thus the average bond distance between them also decreases. However, the larger size particles have a smaller dangling bond with the longer bond distance. The shorter bond length requires more energy as compared to the longer one for absorption. Thus, the absorption is red shifted with the larger particle size. Similar results of increase in the particle size with increase in the pH have been observed in transmission microscopy images.

3.5 Luminescence study

Fig. 8(a) and (b) show the excitation spectra of as-prepared samples of 1, 3, and 7 at.% Sm^{3+} doped GdVO_4 (prepared at

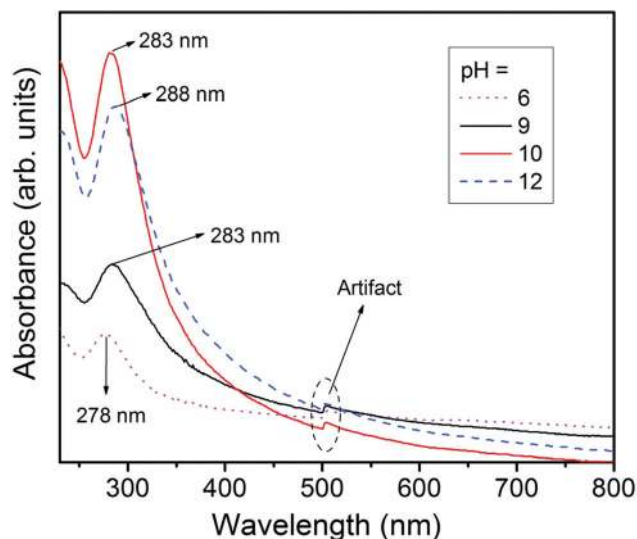


Fig. 7 UV-visible absorption spectra of $\text{GdVO}_4:\text{Eu}^{3+}$ (5 at.%) prepared at different pH.

pH = 12) by monitoring the 646 nm emission and expanded spectra (350–450 nm) to see f–f transitions of Sm^{3+} . A strong peak centered at 310 nm is observed and this is related to the V–O CT band. Apart from these strong peaks we could also observe small peaks above 350 nm. These peaks at 364, 380, 393, 407, 420, 442, and 468 nm correspond to f–f transitions of Sm^{3+} from the ground state $^6\text{H}_{5/2}$ to higher excited states $^4\text{D}_{5/2}$, $^6\text{P}_{7/2}$, $^4\text{G}_{11/2}$, $^4\text{F}_{7/2}$, $^6\text{P}_{5/2}$, $^4\text{G}_{9/2}$ and $^4\text{I}_{13/2}$, respectively.³² However, the absorption peak corresponding to Gd^{3+} electronic transition (S–I transition) at 280 nm could not be distinguished because this peak is merged with V–O CT. It is clearly observed in the spectra that the V–O absorption band is much dominant over the f–f absorptions of the Sm^{3+} . This indicates the occurrence of a strong energy transfer from V–O to Sm^{3+} . Similar observations such as V–O CT and f–f transitions were made for Eu^{3+} , Tm^{3+} and Dy^{3+} doped GdVO_4 samples (not shown).

The energy transfer from VO_4^{3-} absorption to the excited states of activator(s) ($\text{Ln}^{3+} = \text{Dy}^{3+}$, Eu^{3+} , Sm^{3+} , Tm^{3+}) can be explained on the basis of the overlapping of the electric dipole fields of the sensitizer (VO_4^{3-}) and the activator(s). This was introduced by Förster in 1948 and this theory was extended to many systems by Dexter in 1953.^{33,34} VO_4^{3-} can absorb light at 300–320 nm. During this, many electrons are promoted from the ground state to the excited state and thus an equal number of holes is created in the ground state. When the source is removed, electron–hole recombination takes place and gives broad emission from 370 to 500 nm with a maximum at ~ 450 nm.³⁴ It is to be noted that the absorption cross section for VO_4^{3-} is very high ($\alpha = 10^3\text{--}10^5 \text{ cm}^{-1}$), whereas that of Ln^{3+} is $\alpha = 0.1\text{--}10 \text{ cm}^{-1}$ due to the forbidden nature of f–f transition (parity selection rule).³⁵ In addition, emissions of Ln^{3+} ions from Ln_2O_3 have the poor luminescence because of cross-relaxation among Ln^{3+} ions (known as a concentration quenching effect). However, this forbidden nature of f–f transition can be relaxed by the crystal field when the lanthanide (Ln^{3+}) ions (activators) occupy a crystallographic site of a host. Therefore, a few amounts of Ln^{3+} ions (1–2 at.% to ppm level) are doped into semiconductors–insulators in order to reduce cross-relaxation. In $\text{GdVO}_4:\text{Ln}^{3+}$, the excited photons from VO_4^{3-} emission are absorbed by an

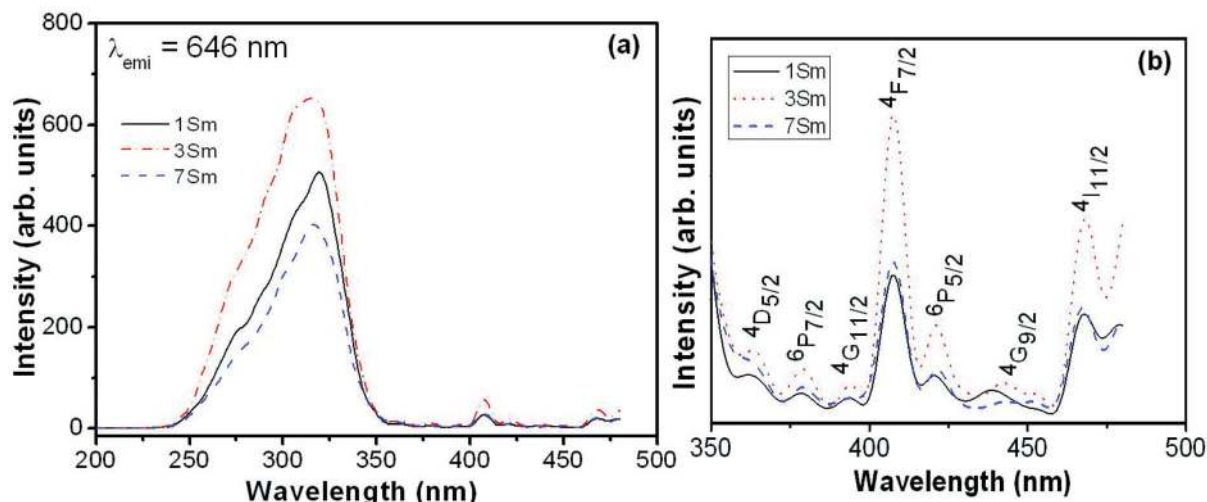


Fig. 8 (a) Excitation spectra of as-prepared samples of 1, 3 and 7 at.% Sm^{3+} doped GdVO_4 , (b) expansion spectra to see f–f transitions of Sm^{3+} .

activator (Ln^{3+}) because the excitation energy levels of Ln^{3+} fall on the emission range of VO_4^{3-} in 370–500 nm. The main excitation–absorption bands of Sm^{3+} , Eu^{3+} , Dy^{3+} and Tm^{3+} are 407, 395 or 467, 355 or 390 and 365 or 390 nm, respectively.^{5–7,14,32,36} Thus the enhancement of luminescence Ln^{3+} doped GdVO_4 is due to energy transfer from VO_4^{3-} to the excited state of Ln^{3+} .

Ln^{3+} ions in GdVO_4 have D_{2d} symmetry. The Gd^{3+} ion forms GdO_8 (dodecahedron) with two different bond lengths in Gd–O . V^{5+} ion forms VO_4 (tetrahedron) with one V–O bond length. The GdO_8 and VO_4 units are linked by sharing two O atoms. Thus Ln^{3+} ions in Gd^{3+} sites are highly asymmetric. It is expected that the intensity of electric dipole transition should be more than that of the magnetic dipole transition. This can be seen in the Eu^{3+} doped sample, where the intensity of electric dipole transition at 615 nm is more than that of magnetic dipole transition at 593 nm. After the absorption of energy at 310 nm through V–O charge transfer, there is direct energy transfer to Ln^{3+} through V–O–Ln^{3+} . The distance between V and Ln^{3+} will be half of the unit cell parameter (a , c), *i.e.*, 3–4 Å, which is much less than that of Förster's maximum distance (20 Å).

3.6 Re-dispersion in the solvent

The as-prepared samples are re-dispersible in solvents such as ethanol, methanol and water. Fig. 9 shows the emission spectra of (a) Dy^{3+} (2 at.%), (b) Eu^{3+} (5 at.%), (c) Sm^{3+} (3 at.%) and (d) Tm^{3+} (2 at.%) particles (prepared at pH = 12) dispersed in ethanol under excitation at 310 nm. All spectra show appreciable luminescence with their respective characteristic peaks. Similarly, same patterns of luminescence are observed when

dispersed in water and methanol (please see ESI, Fig. S4†). Re-dispersion of the particles in these polar solvents is due to the presence of a O–H group on the surface of the prepared particles from the capping agent (EG–PEG). The O–H group of EG–PEG can make hydrogen bonding with the polar solvents. And the presence of a O–H group on the surface of the particles was confirmed by the FTIR study. Fig. 10(a) shows photographs of dispersed samples in water under direct excitation of UV light (using 150 W xenon lamp).

3.7 PVA composite film formation

About 10 mg of Ln^{3+} ($\text{Ln}^{3+} = \text{Dy}^{3+}$, Eu^{3+} , Sm^{3+} , Tm^{3+}) doped GdVO_4 as-prepared samples (prepared at pH = 12) are dispersed in 10 ml of deionized water separately and the dispersion remains for 3 days. Five millilitres of the dispersed solution was mixed with 10 ml of 4% PVA solution (*i.e.* 4 g of PVA in 100 ml deionized water). After being thoroughly mixed in an ultrasonic bath, it was treated with 1 ml of 0.1 M solution of borax. Then the polymer composite film was prepared over a glass slide with film thickness of ~1 mm. Characteristic emission lines of dispersed solutions and polymer films of Ln^{3+} doped GdVO_4 are also observed under excitation of 310 nm. The photographic pictures of composite films under UV irradiation are shown in Fig. 10(b). They give characteristic colours of light emission. In both cases bright red (Eu^{3+}), orange (Sm^{3+}) and blue (Tm^{3+}) are observed whereas we observe a nearly green color for Dy^{3+} which may be due to the mixture of blue and yellow emissions of the Dy^{3+} . This is direct evidence of the importance of re-dispersible particles. Moreover, such re-dispersible particles could be quite useful for biological applications and polymer based

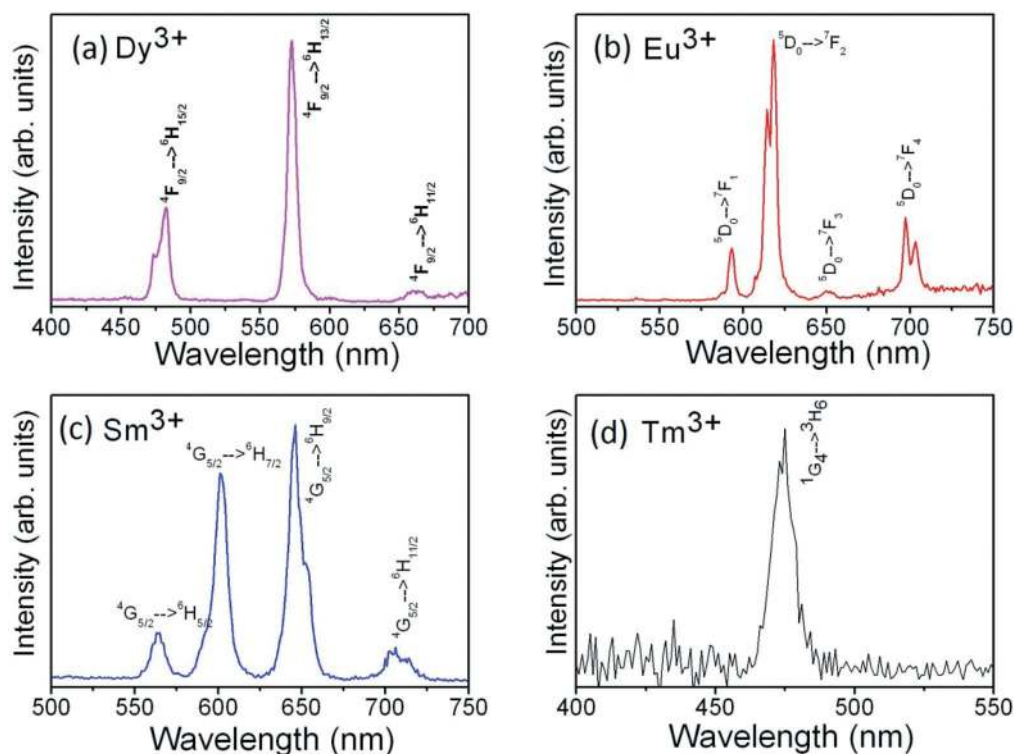


Fig. 9 Emission spectra of as-prepared GdVO_4 doped with (a) Dy^{3+} (2 at.%), (b) Eu^{3+} (5 at.%), (c) Sm^{3+} (3 at.%) and (d) Tm^{3+} (2 at.%) after re-dispersion in ethanol. The excitation wavelength is 310 nm.

luminescent materials. The possible film formation is related to cross-linked complexation between PVA molecules by borax, which is shown schematically here (Fig. 10(c)). Such cross-link between PVA and borax was reported.^{37,38} The film formation with the samples was further confirmed using an FTIR study (see ESI, Fig. S5†).

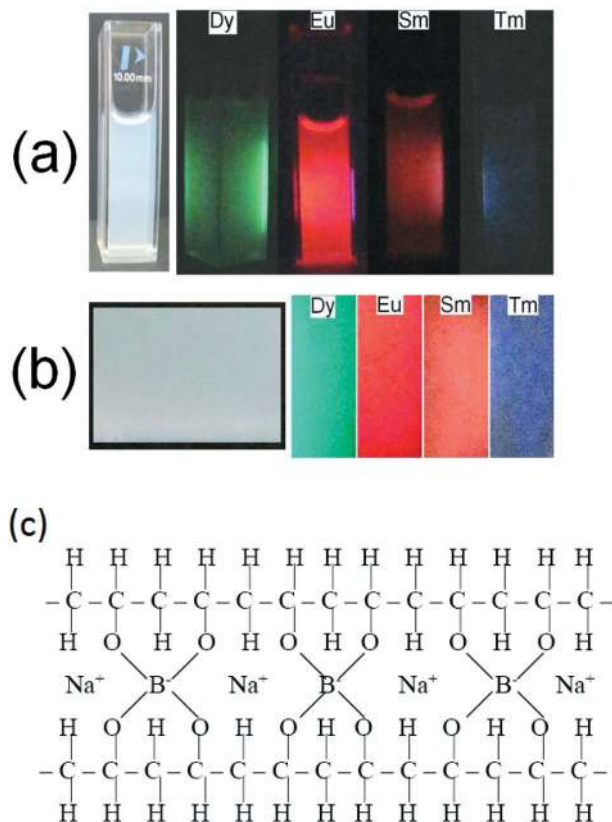


Fig. 10 Photographs of (a) dispersed samples of $\text{GdVO}_4:\text{Ln}^{3+}$ ($\text{Ln}^{3+} = \text{Dy}^{3+}, \text{Eu}^{3+}, \text{Sm}^{3+}, \text{Tm}^{3+}$) and (b) polymer films after incorporation of dispersed particles in polyvinyl alcohol under UV irradiation and (c) schematic representation of PVA linkage with borax.

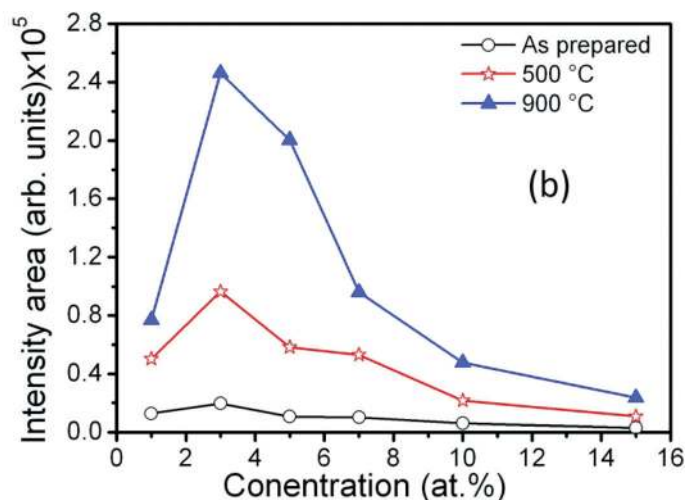
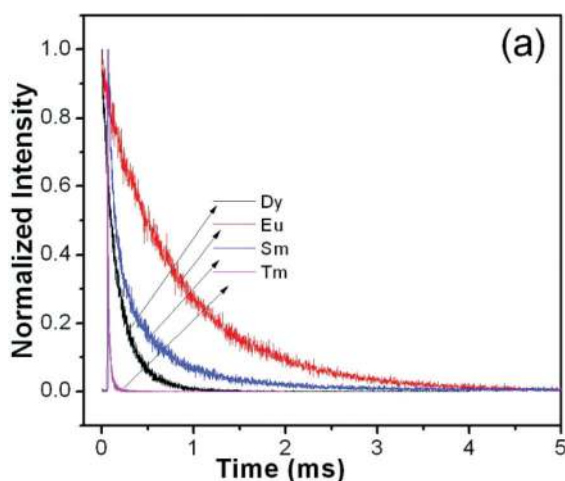


Fig. 12 Luminescence decay curves of GdVO_4 doped with Dy^{3+} (2 at.%), Eu^{3+} (5 at.%), Sm^{3+} (3 at.%) and Tm^{3+} (2 at.%) after dispersion in water. (b) Intensity area versus Sm^{3+} concentrations for the as-prepared, 500 and 900 °C heated samples.

3.8 Effect of the pH on luminescence

Fig. 11 shows the pH dependence on luminescence emission intensity of 5 at.% Eu^{3+} doped GdVO_4 . The samples were prepared at a concentration of 1 mg ml^{-1} (methanol). From the PL study it is observed that the intensity is found to increase with increasing the pH and a maximum is found for samples prepared at pH = 12. This is due to the fact that at low pH the particles are small and the surface to volume ratio is greater and thereby the extent of the non-radiative transition rate is greater as compared to the larger particles prepared at higher pH.

3.9 Luminescence decay

Fig. 12(a) shows the luminescence decay curves of $\text{GdVO}_4:\text{Ln}^{3+}$ ($\text{Ln}^{3+} = \text{Dy}^{3+}, \text{Eu}^{3+}, \text{Sm}^{3+}, \text{Tm}^{3+}$) samples (prepared at pH = 12) dispersed in water having respective dopings of 2, 5, 3, 3

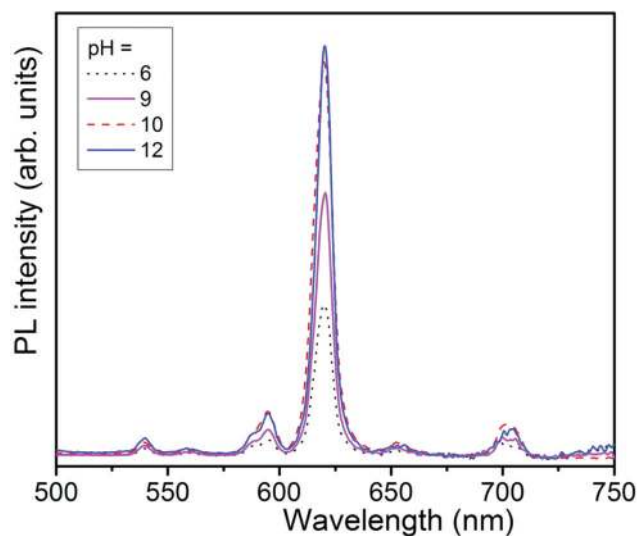


Fig. 11 PL emission spectra of $\text{GdVO}_4:\text{Eu}^{3+}$ (5 at.%) prepared at different pH.

Table 1 Luminescence decay lifetimes of as-prepared, 500 and 900 °C heated samples of GdVO₄: Sm³⁺

Sample no.	Sample name	Luminescence decay lifetime (τ, μs)		
		As-prepared	500 °C	900 °C
1	Gd _{0.99} Sm _{0.01} VO ₄	5.0	520	600
2	Gd _{0.97} Sm _{0.03} VO ₄	5.7	580	660
3	Gd _{0.95} Sm _{0.05} VO ₄	4.7	410	470
4	Gd _{0.93} Sm _{0.07} VO ₄	4.4	240	300
5	Gd _{0.90} Sm _{0.10} VO ₄	3.7	130	150
6	Gd _{0.85} Sm _{0.15} VO ₄	2.3	29	50

and 2 at.%. All luminescence decay data are fitted with biexponential and their mean lifetime values are found to be 190, 883, 280 and 6 μs, respectively. The reported lifetime values of GdVO₄ doped with Dy³⁺ (2 at.%), Eu³⁺ (7 at.%), Sm³⁺ (3 at.%) and Tm³⁺ (2 at.%) were 114, 459, 370 and 13 μs, respectively.^{5–7,39}

In order to study the effects from the heat treatment and concentrations of Sm³⁺ doped GdVO₄ samples (prepared at pH = 12), the integrated area under the curves of as-prepared, 500 and 900 °C samples is calculated using

$$I = \int_{\lambda_1}^{\lambda_2} I(\lambda) d\lambda \quad (1)$$

From Fig. 12(b), it is observed that emission intensity increases with Sm³⁺ concentrations up to 3 at.% and thereafter it is found to decrease with the increase of concentration due to the well known concentration quenching effect. Also the emission intensity increases with the increase of heat treatment. This is due to an increase in the crystallinity and removal of organic groups (–OH, –CH₂–) of the capping agent chemically bonded/adsorbed on the surface of the particle because vibration of such groups quenches the luminescence. Enhancement of the luminescence intensity with increase of heat treatment up to 900 °C is also observed in Dy³⁺ or Eu³⁺ or Tm³⁺ doped GdVO₄ samples (see ESI, Fig. S6†). The lifetime increases with increasing the heat-treatment temperature (Table 1). This is related to the extent of reduction of non-radiative transition probability, which arises from the surface of the particles.

4. Conclusions

Crystalline GdVO₄ nanoparticles doped with Ln³⁺ (Ln³⁺ = Dy³⁺, Eu³⁺, Sm³⁺, Tm³⁺) have been successfully prepared using EG-PEG at relatively low temperature. The transmission electron microscopy image indicates well-dispersed particles. The pH dependence on the particle size gives a new direction for the preparation of different particle sizes. These samples are well dispersible in polar solvents such as ethanol, methanol and water. Further, they have been successfully incorporated in a PVA polymer matrix. For maximum luminescence, the optimum concentration of Sm³⁺ in GdVO₄ is found to be 3 at.%. From the luminescence and its decay studies, the decrease in non-radiative transition probability with the heat treatment is reported.

Acknowledgements

N. Shanta Singh thanks CSIR, New Delhi for senior research fellowship.

References

- G. Blasse and B. C. Grabmaier, *Luminescent Materials*, Springer, Berlin, 1994.
- G. Blasse, *J. Chem. Phys.*, 1966, **45**, 2356.
- J. W. Stouwdam and F. C. J. M. van Veggel, *Nano Lett.*, 2002, **2**, 733.
- E. A. Manders and L. G. Deshazer, *J. Opt. Soc. Am.*, 1971, **61**, 684.
- N. Shanta Singh, R. S. Ningthoujam, L. R. Devi, N. Yaiphaba, V. Sudarsan, S. D. Singh, R. K. Vatsa and R. Tewari, *J. Appl. Phys.*, 2008, **104**, 104307.
- N. Shanta Singh, R. S. Ningthoujam, N. Yaiphaba, S. D. Singh and R. K. Vatsa, *J. Appl. Phys.*, 2009, **105**, 064303.
- N. Shanta Singh, R. S. Ningthoujam, S. D. Singh, B. Viswanadh, N. Manoj and R. K. Vatsa, *J. Lumin.*, 2010, **130**, 2452.
- G. Li, Z. Wang, M. Yu, Z. Quan and J. Lin, *J. Solid State Chem.*, 2006, **179**, 2698.
- X. He, L. Zhang, G. Chen and Y. Hang, *J. Alloys Compd.*, 2009, **467**, 366.
- L. R. Singh, R. S. Ningthoujam, V. Sudarsan, I. Srivastava, S. D. Singh, G. K. Dey and S. K. Kulshreshtha, *Nanotechnology*, 2008, **19**, 055201.
- W. Wang, M. Yu, C. K. Lin and J. Lin, *J. Colloid Interface Sci.*, 2006, **300**, 176.
- K. Riwotzki and M. Haase, *J. Phys. Chem. B*, 1998, **102**, 10129.
- K. Riwotzki and M. Haase, *J. Phys. Chem. B*, 2001, **105**, 12709.
- N. Shanta Singh, R. S. Ningthoujam, M. N. Luwang, S. D. Singh and R. K. Vatsa, *Chem. Phys. Lett.*, 2009, **480**, 237.
- R. S. Ningthoujam, R. Shukla, R. K. Vatsa, V. Deppel, L. Kienle and A. K. Tyagi, *J. Appl. Phys.*, 2009, **105**, 084304.
- H. Wang, C. K. Lin, X. M. Liu, J. Lin and M. Yu, *Appl. Phys. Lett.*, 2005, **87**, 181907.
- J. W. Stouwdam and F. C. J. M. van Veggel, *Langmuir*, 2004, **20**, 11763.
- G. Phaomei, R. S. Ningthoujam, W. R. Singh, N. Shanta Singh, M. N. Luwang, R. Tewari and R. K. Vatsa, *Opt. Mater.*, 2010, **32**, 616.
- M. N. Luwang, R. S. Ningthoujam, Jagannath, S. K. Srivastava and R. K. Vatsa, *J. Am. Chem. Soc.*, 2010, **132**, 2759.
- N. Yaiphaba, R. S. Ningthoujam, N. Shanta Singh, R. K. Vatsa and N. R. Singh, *J. Lumin.*, 2010, **130**, 174.
- G. G. Pan, H. W. Song and X. Bai, *J. Phys. Chem. C*, 2007, **111**, 12472.
- W. Xu, Y. Wang and X. Bai, *J. Phys. Chem. C*, 2010, **114**, 9975.
- L. P. Xie, H. W. Song and Y. Wang, *J. Phys. Chem. C*, 2010, **114**, 14018.
- L. Qu and X. Peng, *J. Am. Chem. Soc.*, 2002, **124**, 2049.
- B. O. Dabbousi, J. Rodriguez-Viejo, F. V. Mikulec, J. R. Heine, H. Mattoussi, R. Ober, K. F. Jensen and M. G. Bawendi, *J. Phys. Chem. B*, 1997, **101**, 9463.
- D. V. Talapin, J. H. Nelson, E. V. Shevchenko, S. Aloni, B. Sadtler and A. P. Alivisatos, *Nano Lett.*, 2007, **7**, 2951.
- J. Livage, *Materials*, 2010, **3**, 4175.
- J. A. Dean, *Lange's Handbook of Chemistry*, McGraw-Hill, 1999.
- H. Wu, H. Xu, Q. Su, T. Chen and M. Wu, *J. Mater. Chem.*, 2003, **13**, 1223.
- M. Chang and S. Tie, *Nanotechnology*, 2008, **19**, 075711.
- L. Sun, Y. Zhang, J. Zhang, C. Ya, C. Liao and Y. Lu, *Solid State Commun.*, 2002, **124**, 35.
- E. Cavalli, A. Belletti, R. Mahiou and P. Boutinaud, *J. Lumin.*, 2010, **130**, 733.
- Th. Förster, *Ann. Phys.*, 1948, **2**, 55.
- D. L. Dexter, *J. Chem. Phys.*, 1953, **21**, 836.
- R. S. Ningthoujam, in *Enhancement of Luminescence by Rare Earth Ions Doping in Semiconductor Host*, ed. S. B. Rai and Y. Dwivedi, Nova Science Publications, USA, 2012, ch. 7.
- L. R. Singh and R. S. Ningthoujam, *J. Appl. Phys.*, 2010, **107**, 104304.
- H.-L. Lin, T. L. Yu and C.-H. Cheng, *Colloid Polym. Sci.*, 2000, **278**, 187.
- C. Y. Chen, J. Y. Guo, T. L. Yu and S. C. Wu, *J. Polym. Res.*, 1998, **5**, 67.
- F. Zheng, E. Wang and P. Yang, *Optoelectron. Adv. Mater.*, 2011, **5**, 596.